Heliyon 10 (2024) e35442

Contents lists available at ScienceDirect

Heliyon

journal homepage: www.cell.com/heliyon

Research article

BRF1 promotes the odontogenic differentiation of dental pulp stem cells in pulpitis by inducing autophagy

Caixia Zhou [a,b,c,d,1], Yan Wu [a,b,c,1], Yizhen Teng [a,b,c], Jian Zhang [a,b,c], Jiarong Liu [a,b,c,*]

[a] Department of Stomatology, Union Hospital, Tongji Medical College, Huazhong University of Science and Technology, Wuhan, 430022, China
[b] School of Stomatology, Tongji Medical College, Huazhong University of Science and Technology, Wuhan, 430030, China
[c] Hubei Province Key Laboratory of Oral and Maxillofacial Development and Regeneration, Wuhan, 430022, China
[d] Now Working in Shenzhen Stomatological Hospital, Shenzhen, 518000, China

ARTICLE INFO

Keywords:
Autophagy
BRF1
LC3
Pulpitis
Stem cells

ABSTRACT

Objective: While post-transcriptional modifications play a pivotal role in the autophagy regulation, studies on dental pulp disease are limited. This study investigated the effect of BRF1 on autophagy in inflamed pulp tissue and human dental pulp stem cells (hDPSCs).
Methods: Immunohistochemical analysis was used to examine BRF1 expression, autophagy levels, and dentinogenic markers in normal and inflamed pulp. The presence of autophagosomes was observed by transmission electron microscopy. Primary hDPSCs were treated with 1 μg/mL lipopolysaccharide (LPS) for different lengths of time. The expression of BRF1 and autophagy makers was determined by Western blotting. BRF1 knockdown and 3 MA treatment were employed to assess changes in autophagy and dentinogenic differentiation. Double immunofluorescence staining was performed to co-localize BRF1 with LC3B in pulp tissue.
Results: The expressions of BRF1, LC3, DMP1, and DSP were significantly elevated in the inflamed pulp. LPS enhanced the protein production of IL-6, BRF1, LC3, and Beclin-1 from 6 h to 24 h after the treatment. BRF1 knockdown reduced the ratio of LC3-II/LC3-I and the differentiation ability of hDPSCs, while 3 MA inhibited LPS-mediated dentinogenic differentiation. Double-labeling revealed that BRF1 co-localized with LC3B in inflamed pulp.
Conclusion: This study demonstrated that BRF1 promoted autophagy activation and odontogenic differentiation in pulpitis.

1. Introduction

Dental pulp stem cells (DPSCs) refer to a subset of undifferentiated cells that can regenerate a dentin/pulp-like complex, with their multipotent potential influenced by various irritants. Autophagy is an evolutionarily conserved process by which cells break down their own damaged components to achieve cellular homeostasis and renovation [1]. Mounting evidence indicates that autophagy is implicated in the differentiation of mesenchymal stem cells and dental precursor cells during enamel and dentin formation [2]. At the cellular level, autophagic activation and levels vary depending on cell types and stimuli [2–4]. Our previous work demonstrated that

* Corresponding author. Address 1277# Jiefang avenue, Wuhan, Hubei Province, China.
E-mail addresses: 525475617@qq.com (C. Zhou), 544356836@qq.com (Y. Wu), kqyyljr@aliyun.com (J. Liu).
[1] These authors share first authorship.

https://doi.org/10.1016/j.heliyon.2024.e35442
Received 15 June 2024; Received in revised form 26 July 2024; Accepted 29 July 2024
Available online 30 July 2024

autophagy was involved in the PRP-induced migration, proliferation, and differentiation of pulp fibroblasts, suggesting that phagocytic activation could promote pulp regeneration [5].

The mechanism by which inflammation-related signals regulate autophagy is multi-factorial [1,6]. The autophagic process is mediated via coordinated actions of various autophagy-related factors, such as Beclin-1, autophagy protein 5 (ATG5), and microtubule-associated proteins light chain 3 (LC3). These factors are regulated through multiple steps, including post-transcriptional regulation of mRNA stability, a crucial event of gene expression [7].

Butyrate response factor 1 (BRF1) belongs to a class of RNA-binding proteins known as the ZFP36 protein family, which bind to the AU-rich elements (AREs) in the 3' UTR regions of the target mRNA, facilitated by its zinc finger domains. This binding interaction leads to mRNA destabilization [8]. Recent studies have found that ZFP36 proteins, including BRF1, exert significant role over cellular response to lipid peroxidation, apoptosis, oxidative stress, and immune stimuli [9,10]. For instance, ZFP36 overexpression in hepatic stellate cells resulted in ATG16L1 mRNA decay by binding to the AREs in the 3'-UTR, thus triggering autophagy inactivation, blocking autophagic ferritin degradation, thereby conferring resistance to ferroptosis [11]. Notably, elevated levels of BRF1 have been associated with accelerated tumorigenesis and modifications in immune infiltration in various cancers, such as prostate cancer [12–16]. Moreover, BRF1 induction plays a crucial role in autophagy activation elicited by globular adiponectin and is a promising target for anti-inflammatory responses [8,17]. However, little is known about its impact on pulp infection. Our hypothesis was that BRF1 might also be a player in the inflammation-induced autophagy in pulp stem cells.

In this study, we investigated the expression of BRF1 and regulation of autophagy in tissue specimens from early-stage pulpitis and isolated human DPSCs. Human dental pulp samples were obtained from third molar teeth with malposition or healthy teeth extracted for orthodontic purposes. The pulpitis group included those with a history of spontaneous and intense pain but without periodontal disease. We also examined the effect of RNA interference and autophagy inhibition on the odontogenic differentiation of hDPSCs.

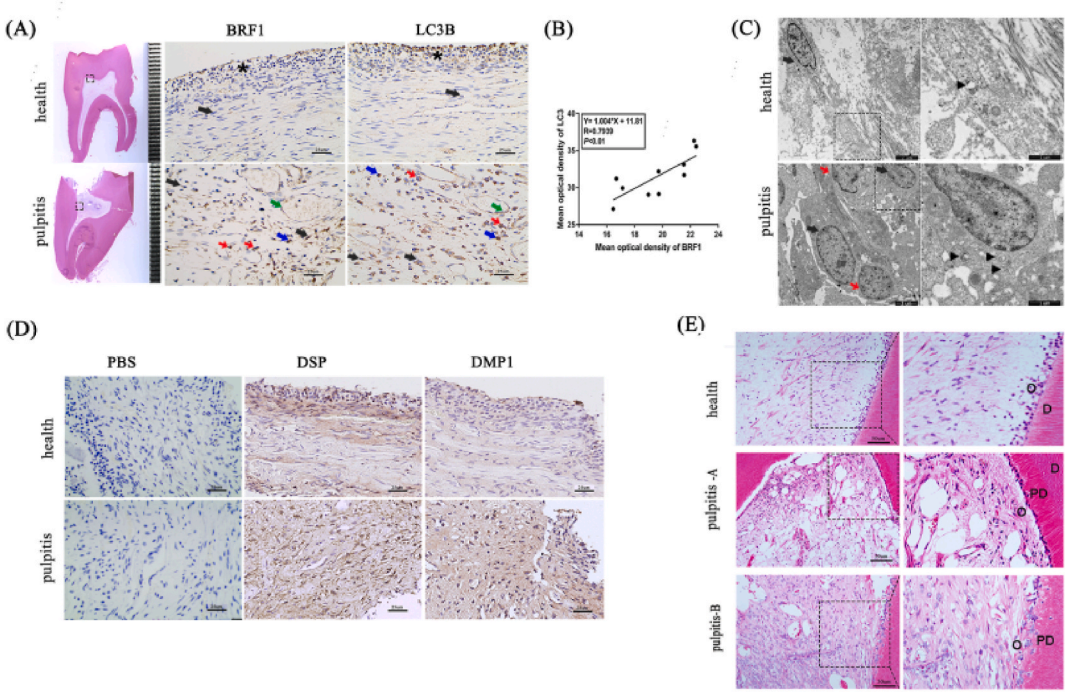

Fig. 1. BRF1, autophagy and dentinogenesis were enhanced in human inflamed pulp by immunohistochemical analysis. Human pulp samples were sorted into health and pulpitis groups (n = 5). (A) In healthy pulp, LC3B and BRF1 positive cells were restricted in the odontoblast layer (black asterisk). In pulpitis, the expression of LC3B and BRF1 in fibroblast-like cells (black arrow) was significantly increased. Neutrophils (red arrow), mononuclear macrophages (blue arrow), and perivascular cells (green arrow) were also positive. Scale bars = 25 μm. (B) LC3B and BRF1 showed a positive correlation by Spearman analysis. (C) The Fibroblast-like cells (black arrow), neutrophils (red arrow), and autophagosomes (black triangle) in dental pulp were observed by transmission electron microscopy. Scale bars = 2 μm (left), Scale bars = 1 μm (right). (D) Expression of DSP and DMP1 were also localized within the pulp. The PBS was the negative control. Scale bars = 25 μm. (E) H&E staining. The pulpitis-A region is a non-inflammatory cell infiltrating area where predentin (PD) was deposited between dentin (D) and odontoblasts(O). Pulpitis-B is an inflammatory cell infiltration area where destruction of the odontoblast layer can be detected. Scale bars = 50 μm.

2. Results

2.1. BRF1, autophagy, and dentinogenesis were enhanced in human-inflamed pulp

We first performed immunohistochemical staining on the inflamed pulp for BRF1 and LC3, comparing their expression pattern with those in normal pulp. The results showed that in inflamed pulp, strong BRF1 and LC3 staining was found in fibroblast-like cells, inflammatory cells, and perivascular cells beneath the sub-odontoblastic layer near the inflammatory site, whereas only limited expression was detected in odontoblasts in normal pulp (Fig. 1A). Spearman analysis indicated a positive correlation between BRF1 and LC3 (Fig. 1B). The presence of autophagosomes in inflamed pulp was confirmed by transmission electron microscopy (Fig. 1C). To assess whether pulp lesion leads to reactionary dentin in pulpitis, the dentin of the teeth was labeled with DMP1 and DSP, and the result showed a higher expression level beneath the odontoblastic layer of inflamed pulp (Fig. 1D). Hematoxylin-eosin staining further revealed extensive deposition of extracellular matrix, and osteo/predentin formation near the exposed pulp, suggesting that inflamed pulp exhibits odontoblastic differentiation and tissue repair capabilities (Fig. 1E).

2.2. LPS induced BRF1 and autophagy in a time-dependent manner in hDPSCs

We treated hDPSCs with LPS *in vitro* to further examine the relationship between BRF1 and autophagy. Isolated hDPSCs were identified by characterization of antigens, including CD34, CD44, CD45, CD73, CD90, and CD105 (Fig. 2A). WB analysis suggested that LPS significantly up-regulated the protein expression of BRF1, LC3II/LC3I, BECN1 and IL6 in a time-dependent manner, while ATG5 remained unchanged during the 0–24 phase (Fig. 2B).

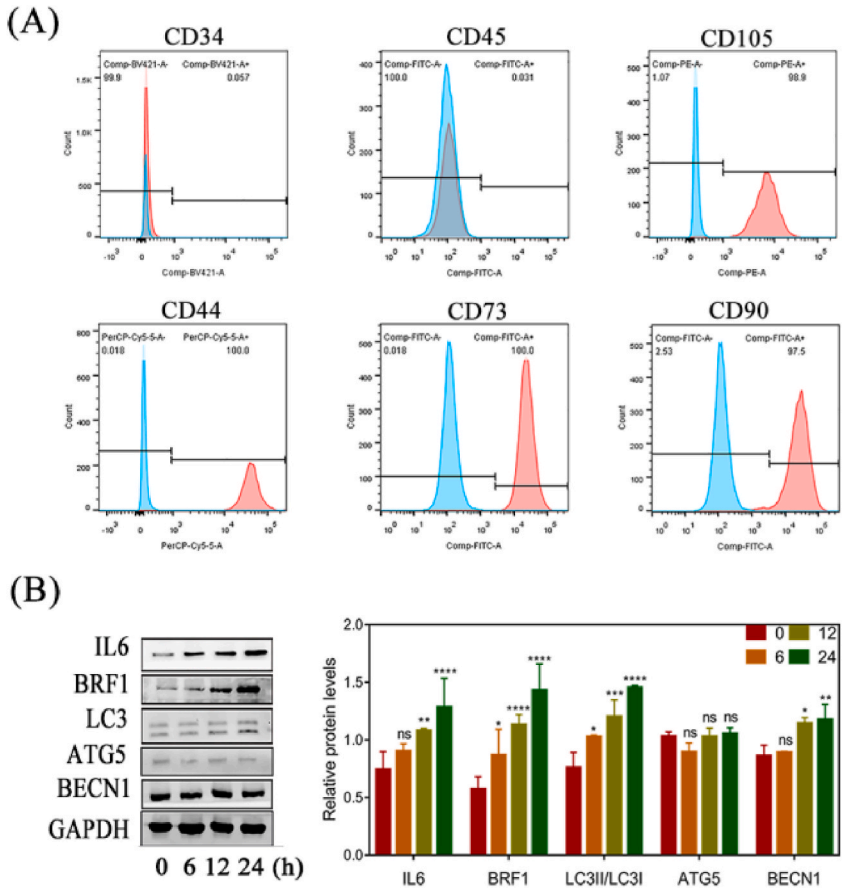

Fig. 2. The expression pattern of BRF1 and autophagy in hDPSCs mediated by LPS in vitro. (A) Surface antigen identification of hDPSCs was detected by flow cytometry. The expression rates of mesenchymal stem cell surface markers CD105, CD44, CD73 and CD90 were positive, and the expression rates were 98.9 %, 100 %, 100 % and 97.5 %, respectively. While the expression of hematopoietic stem cell surface markers CD34 and CD45 was negative, and the expression rates were 0.06 % and 0.03 %, respectively. (B) hDPSCs were cultured with LPS for 6, 12 and 24 h, and the protein of IL6, BRF1, LC3, ATG5 and BECN1 was detected with WB. Quantification of above protein levels using Quantity One®. Experiments were repeated in triplicate. Mean ± SEM, *P < 0.05, **P < 0.01, ***P < 0.001, ****P < 0.0001.

2.3. BRF1 knockdown or 3 MA treatment decreased autophagy and differentiation in LPS-induced hDPSCs

The relationship between BRF1 and autophagy was explored through functional analysis. Cultured hDPSCs were transfected with specific siRNA directed against BRF1. The efficiency of siRNA transfection was confirmed via PCR at mRNA level (Fig. 3A). Interestingly, silencing BRF1 resulted in decreased expression of LC3II/LC3I, while no significant change observed in the expression of ATG5 and BECN1 (Fig. 3B). Moreover, dentinogenic differentiation was examined by immunofluorescent staining of hDPSCs transfected with BRF1 siRNA after 3-d incubation in DM. As shown in Fig. 3C, BRF1 knockdown caused a sharp decline in the expression DSP and DMP1 in DM-cultured cells. The activity of ALP also dropped after 3-d incubation in DM (Fig. 3D). These results suggested that autophagy and dentinogenic differentiation of hDPSCs was, at least partially, regulated by BRF1.

Given the effect of LPS treatment on autophagic activation, it is likely that autophagy might influence the differentiation process under an inflammatory condition. LPS elevated the expression of OPN, OSX, DSP, and LC3II/LC3I in hDPSCs undergoing dentinogenic differentiation. Under the action of 3 MA, an autophagy inhibitor, these molecules were significantly decreased 7-d after osteogenic induction and culture (Fig. 3E-F). ALP staining results were consistent with Western blot findings (Fig. 3G-H), suggesting that autophagy plays a crucial role in dentinogenic differentiation of the inflammatory hDPSCs.

2.4. Co-localization of BRF1 and LC3 in inflamed pulp tissue

Immunofluorescence double staining of pulp tissue sections confirmed a positive association between BRF1 and LC3 in inflamed pulp. Compared with normal pulp (Fig. 4A), both BRF1 and LC3 expression were significantly elevated in inflamed pulp (Fig. 4B). Moreover, positive staining was detected mainly on the fibroblast-like cells. The merged image revealed that most BRF1-positive cells were also stained positive for LC3, indicating a close association between BRF1 and LC3 during pulp inflammation.

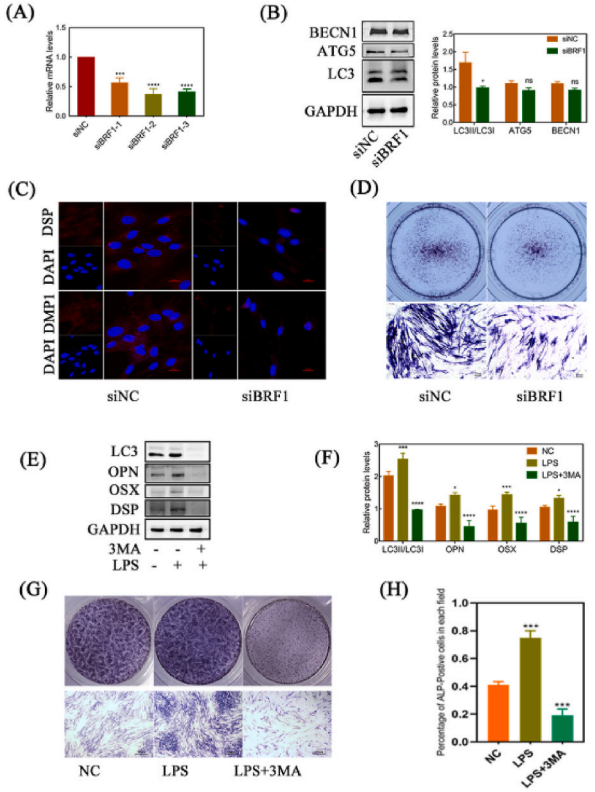

Fig. 3. Autophagy and differentiation of LPS-induced hDPSCs were reduced by BRF1 knockdown or 3 MA treatment.
(A) Three different siBRF1 were measured by PCR, and the siBRF1-2 performed a better inhibitory efficiency. (B) Knockdown of BRF1 by siBRF1-2, the expression of ATG5, BECN1, and the LC3 II/LC3I ratio were examined and quantitated. (C–D) Knockdown of BRF1, DPSCs were cultured with MM for 3 days. IF and ALP were applied to detect the expression of DMP1, DSP, and mineral deposits respectively. Scale bars = 25 μm. (E–F) hDPSCs were cultured in MM, MM + LPS, and MM + LPS+3 MA for 7 days, and the protein of LC3, OPN, OSX and DSP was detected and quantitated. (G) Alkaline phosphatase staining was used to detect mineral deposits in the extracellular matrix in the dishes. Scale bars = 50 μm. (H) The percentage of ALP-positive cells in each field was quantitated. Experiments were repeated in triplicate. Mean ± SEM, *P < 0.05, **P < 0.01, ***P < 0.001, ****P < 0.0001.

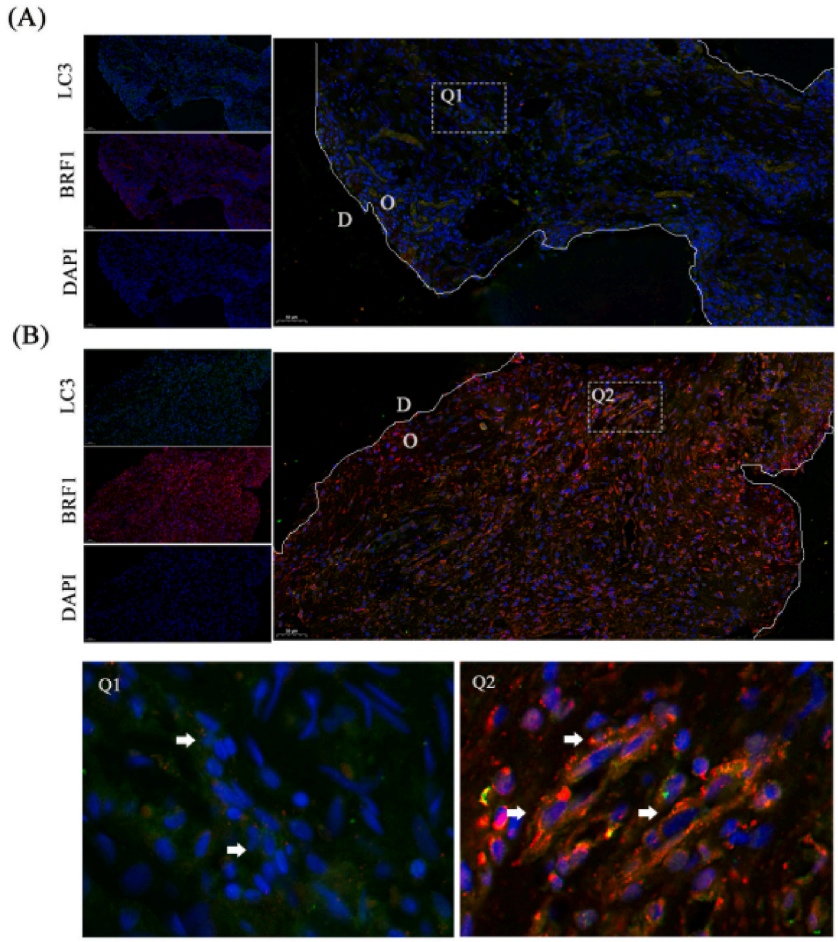

Fig. 4. The co-localization of BRF1 and LC3 in inflamed pulp tissue was achieved by immunofluorescence double-staining. (A) BRF1 (in red) and LC3 (in green) were low expressed in healthy pulp. (B) BRF1 (in red) and LC3 (in green) showed a strong positive stain in the inflamed pulp. Colocalization of BRF1 and LC3 (in yellow) could be observed in fibroblast-like cells (arrow) apart from inflammatory cells. Dentin (D) and odontoblasts (O) were separated by a white curve. Scale bars = 50 μm.

3. Discussion

In this study, BRF1 was first identified to be a potential regulator of autophagy in dental pulpitis. Our data from clinical samples showed a positive correlation between BRF1 expression and LC3 production during the early stage of pulpitis, suggesting a role in pulp repair. Our *in vitro* experiments also demonstrated that BRF1 was involved in autophagy activation and dentinogenic differentiation of hDPSCs under LPS stimulation.

Growing evidence revealed that inflammation is a prerequisite for pulp healing and tissue regeneration [18,19]. High levels of proinflammatory signals accelerate necrosis, apoptosis, and resorption of cells, while low levels of proinflammatory signals trigger differentiation and mineralization. It has been shown that the perivascular stem cells could migrate to the damaged area and form restorative dentin 2 weeks after pulp exposure [20]. Our previous research found that, in irreversible pulpitis, putative pulp stem cells were induced, leaving their quiescent niche to another two specific niches, both adjacent to inflammatory sites [21]. In particular, DPSCs isolated from pulp with irreversible pulpitis exhibited similar or more potent proliferative and multidimensional differentiation than those from healthy pulp, suggesting that DPSCs possess an extraordinary regenerative potential both *in vitro* and *in vivo* [22,23]. Thus, in the present study, we focused on the regenerative role of hDPSCs in pulpitis and explored how autophagy regulates the effect of LPS on hDPSCs.

It has been reported that autophagy is activated in response to stresses and is implicated in the pathogenesis of pulpitis and periapical infection [4,24,25]. Recent studies have provided intriguing insights into the roles of autophagy in tooth development, pulp aging, and stress adaptation [2]. We demonstrated synchronization between autophagy and dentinogenesis in pulpitis, and observed that LPS treatment at 1 μg/mL exerted a positive effect on autophagy activation in hDPSCs. These results were coincident with previous findings, indicating that autophagy protects against inflammation-induced apoptosis in several stem cells [26,27]. Conversely, Lei S et al. reported that a high concentration of LPS downregulated the osteo-/odontogenic differentiation of stem cells from apical papilla

by inducing autophagy [28]. Additional evidence further supports the dual role of autophagy in pre-odontoblastic cells under mild LPS stimulation [29]. These conflicting findings indicated that the core molecules and regulatory mechanism of autophagy warrant further investigation.

In general, we found a positive association between BRF1, autophagy, and dentinogenesis in inflamed pulp. Specifically, LPS stimulation increased the expression levels of BRF1 and autophagy-related molecules, while BRF1 knockdown reduced autophagy of hDPSCs *in vitro*, suggesting that post-transcriptional modifications such as BRF1 play a key part in the regulation of autophagy [7,30]. Autophagy is synergistically governed at both RNA and protein levels. Although numerous transcriptional mediators of autophagy have been identified, post-transcriptional regulation of autophagy is largely unclarified. BRF1 destabilizes target mRNAs by binding 3'-UTR AREs and recruiting deadenylation and degradation factors [31]. The AREs facilitate post-transcriptional control of a wide array of biological functions, including signal transduction, cytokine expression, apoptosis, and oxidative stress [8,17]. A transcriptome-wide study identified TTP, another family member related to BRF1, caused profound changes in the transcriptome and translatome, and altered NF-κB-activation [32].[27] Additionally, BRF1 and TTP regulate autophagy flux in macrophages and hepatic stellate cells, respectively [11,33]. While the molecular link between BRF1 and autophagy signaling pathways is not fully elucidated, these findings collectively suggested that BRF1 plays a role in autophagy regulation under specific physiological stresses.

Additionally, we found that, upon LPS stimulation, autophagy-related molecules LC3II/LC3I and BECN1 were significantly up-regulated, while the change in ATG5 expression was not statistically significant. In the process of autophagy, the Atg5–Atg12/Atg16 complex is essential for the phagophore membrane elongation [34]. A previous study showed that LC3 and BECN1 were time-dependently regulated and increased substantially from day 3 onward, while ATG5 was only marginally elevated and peaked at day 7 after LPS stimulation [29]. This finding suggests that different from LC3, ATG5 might respond to inflammation with a delay. After BRF1 was knocked down, LC3II/LC3I was significantly down-regulated, and BECN1 and ATG5 had a trend of down-regulation, but such downward change was not statistically significant. In hepatic stellate cells, ZFP36 plasmid promoted ATG16L1 mRNA decay, while Ad-BRF1 infection variously impacts the mRNA expression of BECN1, LC3, and ATG7 in macrophages [11,33]. These data suggest that BRF1-regulated autophagy varies substantially across different cell types.

The study sheds light on the intricate relationship between BRF1, autophagy markers (LC3), and dentinogenic markers (DMP1 and DSP), indicating the role of autophagy dysregulation in the pathogenesis of dental pulp disease. Future research could investigate strategies to modulate BRF1 levels or targeting its interactions with autophagy pathways, for managing inflammation and promoting tissue regeneration in dental care. In addition, moving from experimental models to clinical applications represents a significant gap. Further studies are needed to validate findings in human samples and explore the feasibility of targeting BRF1 for therapeutic interventions in dental clinics.

However, the following limitations of this study should be considered, which include 1) the limited sample size of teeth with pulpitis may compromise the statistical power of correlation analysis. As a result, these findings can't be extrapolated to broader populations or geographic regions. 2) the precise mechanisms by which BRF1 modulate autophagy and dentinogenesis in dental pulp remains to be elucidated. Establishing BRF1-overexpressing or BRF1-silenced cell lines would enable detailed investigations into its functional impact.

4. Conclusion

Taken together, the findings of the present study revealed that BRF1 was intimately related to autophagy at the early stage of dental pulpitis and functioned as a positive defense by regulating autophagy. However, further studies are needed to investigate the underlying mechanism of BRF1 at the molecular level and the complex landscape of autophagy during pulp homeostasis.

5. Materials and methods

5.1. Primary cell cultures

Non-diseased pulp tissues of caries-free third molars, extracted from 18- to 22-year-old patients, were used. Studies involving patients received approval from the Medical Ethics Committee of Union Hospital affiliated to Tongji Medical College, Huazhong University of Science and Technology, and were performed in strict accordance with relevant guidelines and regulations. Written informed consent was obtained from all participants. Dental pulp tissues were minced and digested with 4 mg/mL dispase (Gibco, USA) and 3 mg/mL collagenase type I (Invitrogen Life Technology, USA) for 40 min at 37 °C. After centrifugation, digested mixtures

Table 1
Antibodies for Flow cytometry.

name	Art.No.	manufacturers
Hu CD90 FITC 5E10	555595	BD Pharmingen
Hu CD105 PE 266	560839	BD Pharmingen
Hu CD44 PerCP-Cy5.5 G44-26	560531	BD Pharmingen
Hu CD73 APC AD2	560847	BD Pharmingen
Hu CD34 BV421 581	562577	BD Pharmingen
ANTI-Hu CD45 HI30 APC-EF780	47-0459-41	eBioscience

were resuspended in α-MEM (Cyagen, China) supplemented with 20 % fetal bovine serum (FBS, Gibco, USA), 10 mg/mL streptomycin and 10 U/mL penicillin (Sigma, USA), and then seeded into 6-well plates (BEAVER, China). Cells were cultured at 37 °C in a humidified atmosphere of 5 % CO_2. When reaching 80 % confluence, the cells were digested and expanded for the subsequent experiments. Cells at passages 3 to 5 were employed in this study.

5.2. Flow cytometry

The third passage of hDPSCs in the logarithmic growth phase was used. Digested cell pellets were suspended in 10 mL of sterile PBS w/o Ca^{2+} and Mg^{2+} at a density of 1×10^5~5×10^5 cells/mL. Then every 100 μL cell suspension was subjected to incubation with eight different antibodies (Table 1), respectively, for 25 min at 4 °C in the dark. Cells were washed with BD Lyse Wash Assistant kept on ice and analyzed within 2 h of processing after a 10-min incubation with 7-AAD.

5.3. LPS/3 MA treatment and differentiation

Cells were incubated with α-MEM containing 10 % FBS and 1 μg/mL LPS (Sigma, USA) for 0, 6, 12 and 24 h. To examine the potential effect of autophagy on the dentinogenic differentiation, hDPSCs were cultured for 7 days with MM (dentinogenic medium containing 100 nM dexamethasone, 10 mM β-glycerophosphate and 0.2 mM ascorbic acid (Sigma, USA)), MM + LPS, MM + LPS+3 MA (5 mM, MCE, China) respectively.

5.4. Immunofluorescence staining

Cells were seeded evenly onto slides in complete medium. After transfected with siBRF1 or siNC, cells were grown in MM for 3 days. Then the medium was removed, cells were successively rinsed with PBS, fixed with 4 % paraformaldehyde (PFA), and permeabilized with 0.5 % Triton X-100. Upon application of 5 % bovine serum albumin to block the nonspecific antibody-binding sites, the slides were incubated at 4 °C overnight with antibodies against DSP (1:100, sc-73632, Santa Cruz, China) and DMP1 (1:100, sc-73633, Santa Cruz, China), and then with secondary antibody conjugated with Fluor Cy3. Nuclei were stained with DAPI. Images were taken by using a confocal laser scanning microscope.

5.5. Western blot analysis

Protein extractions from cells were measured by utilizing the BCA Protein Assay Kit (Beyotime Biotechnology, China). A similar amount of protein was fractionated by electrophoresis on 15 % or 10 % sodium dodecyl sulfate polyacrylamide gel. It is then cut according to the molecular weight of the target protein and transferred to 0.45-μm polyvinylidene difluoride membranes. After blockade with 5 % non-fat milk at room temperature (RT) for 1 h, the membranes were probed at 4 °C overnight with the following primary antibodies: BRF1 (1:2000, 12306-1-AP, Proteintech, China), LC3B (1:1000, A7198, Abclonal, China), BECN1 (1:1500, A7353, Abclonal, China), ATG5 (1:2000, A0203, Abclonal, China), IL6 (1:600, ab6672, Abcam, USA), OPN (1:1000, 22952-1-AP, Proteintech, China), DSP(1:1000, A8413, Abclonal), OSX(1:1000, ab209484, Abcam). After washing three times with TBST, the membranes were incubated with anti-rabbit/mouse secondary antibody for 1 h at RT. Afterwards, reactive signals of membranes were detected by exposing them to autoradiographic film (Amersham, UK) supplemented with enhanced chemiluminescence substrate reagent (Millipore, USA).

5.6. Alkaline phosphatase assay

Cells were treated as needed. After rinsing 3 times with PBS, the cells and matrices in 24-well plates were fixed with 4 % paraformaldehyde (PFA) for 15 min, and then stained with BCIP/NBT Alkaline Phosphatase Color Development Kit (Beyotime Biotechnology, China) to detect mineral deposits in the extracellular matrix.

5.7. Small interfering RNA transfection

Small inhibitory RNA against BRF1 (siBRF1, Gene Pharma, China) was used to interfere BRF1 expression. Cells were cultured in six-well plates and transfected with 40 nm BRF1-targeted siRNA and the universal negative control siRNA (siNC) by using Lipofectamine3000 reagent (Lipo3000) (Invitrogen, USA) according to the manufacturer's instructions. Silencing efficacy was checked by polymerase chain reaction (PCR) 24 h after transfection. For alkaline phosphatase detection and Western blotting, cells were grown in MM for 3 days, after transfection with siBRF1 or siNC.

5.8. Dental pulp samples from patients

Third molar teeth from patients aged 18–45 were employed in this study. These samples contained 9 healthy teeth and 9 pulpitis teeth caused by caries. All of them were collected from the Department of Stomatology, Union Hospital, Wuhan, China. For histological analysis, samples were decalcified with 10 % EDTA for 4 months after fixation with 4 % PFA, then paraffin-embedded and prepared into 3–5 mm sections.

5.9. Transmission electron microscopy

Healthy and inflammatory pulp tissues from patients were fixed in 2.5 % glutaraldehyde buffer pre-cooled at 4 °C. These samples were successively fixed in 1 % osmium tetroxide for 1 h, dehydrated in graded ethanol and propylene oxide, embedded in Epon-812, cut into sections by ultramicrotome, and stained with lead citrate and uranyl acetate. Finally, images were obtained by transmission electron microscopy (FEI Tecnai G20 TWIN, USA) at an accelerating voltage of 200 kV.

5.10. Immunohistochemical and immunofluorescence staining

For histological analysis, sections were stained with H&E (Sigma, USA). For immunohistochemical staining, the sections were dewaxed with xylene and hydrated with graded ethanol. After antigen retrieval by microwave heating with sodium citrate buffer, sections were incubated with anti-BRF1 antibody (1:100, 12306-1-AP, Proteintech, China), anti-LC3B antibody (1:100, A7198, Abclonal, China), anti-DSP antibody (1:100, sc-73632, Santa Cruz, China), and anti-DMP1 antibody (1:100, sc-73633, Santa Cruz, China) at 4 °C overnight. Meanwhile, Ultrasensitive TM SP (mouse/rabbit) IHC Kit (MXB, China) and DAB Kit (MXB, China) were applied by following the manufacturer's instructions. Nuclei were stained with hematoxylin (Beyotime Biotechnology, China). After dehydration with graded ethanol and transparentized with xylene, sections were enveloped with neutral resin size (MXB, China). ImageJ software was used for protein quantification. For immunofluorescence double staining, the procedure was the same as that of immunohistochemistry before antigen retrieval. Then the sections were incubated at 4 °C overnight with antibodies against LC3B (1:100, A17424, Abclonal, China) and BRF1 (1:50, 12306-1-AP, Proteintech, China), and then with secondary antibody conjugated with Fluor Cy3 or 488. Nuclei were stained with DAPI. Images were taken by using a fluorescence microscope.

5.11. Real-Time PCR

Total RNA was extracted from hDPSCs by using Trizol reagents (Vazyme Biotechnology), and reversely transcribed to cDNA with a reverse transcription kit (Vazyme Biotechnology) according to the manufacturer's instructions. Real-time PCR was performed on a StepOne™ Real-Time PCR System (Applied Biosystems) by using AceQ Universal SYBR qPCR Master Mix (Vazyme Biotechnology). Primers were designed as follows: BRF1 (forward: GACCACCACCCTCGTGTCT, reverse: GGTGCCCACTGCCTTTCT), GAPDH (forward: ATTCCATGGCACCGTCAAGG, revers : TCGCCCCACTTGATTTTGGA). Finally, the mRNA expression levels were analyzed by delta-delta CT.

5.12. Statistical analysis

All data were presented as mean ± standard deviation (SD). Graphs and associated statistical analyses were performed by using GraphPad Prism 7.0. Statistically significant differences ($P < 0.05$) were assessed by a Two-tailed *t*-test and ANOVA. All experiments were repeated at least 3 times.

Data availability statement

The authors confirm that the data supporting the findings of this study are available within the article [and/or] its supplementary materials.

CRediT authorship contribution statement

Caixia Zhou: Project administration, Methodology, Investigation, Formal analysis, Data curation. **Yan Wu:** Formal analysis, Data curation. **Yizhen Teng:** Software, Resources. **Jian Zhang:** Validation, Supervision. **Jiarong Liu:** Funding acquisition, Conceptualization.

Declaration of competing interest

The authors declare that they have no known competing financial interests or personal relationships that could have appeared to influence the work reported in this paper.

Acknowledgment

I would like to thank Professor Yuan and Professor Tang, for their valuable guidance throughout my studies. You provided me with the tools that I needed to choose the right direction and successfully complete my dissertation.

Appendix A. Supplementary data

Supplementary data to this article can be found online at https://doi.org/10.1016/j.heliyon.2024.e35442.

References

[1] V. Deretic, Autophagy in inflammation, infection, and immunometabolism, Immunity 54 (2021) 437–453.
[2] S. Yang, W. Fan, Y. Li, Q. Liu, H. He, F. Huang, Autophagy in tooth: physiology, disease and therapeutic implication, Cell Biochem. Funct. 39 (2021) 702–712.
[3] S. Qi, et al., Expression of autophagy associated proteins in rat dental irreversible pulpitis, Mol. Med. Rep. 19 (2019) 2749–2757.
[4] H.S. Wang, F. Pei, Z. Chen, L. Zhang, Increased apoptosis of inflamed odontoblasts is associated with CD47 loss, J. Dent. Res. 95 (2016) 697–703.
[5] H. Xu, F. Xu, J. Zhao, C. Zhou, J. Liu, Platelet-rich plasma induces autophagy and promotes regeneration in human dental pulp cells, Front. Bioeng. Biotechnol. 9 (2021) 659742.
[6] N. Mizushima, M. Komatsu, Autophagy: renovation of cells and tissues, Cell 147 (2011) 728–741.
[7] Q. Ma, S. Long, Z. Gan, G. Tettamanti, K. Li, L. Tian, Transcriptional and post-transcriptional regulation of autophagy, Cells 11 (2022).
[8] F.E. Tan, M.B. Elowitz, Brf1 posttranscriptionally regulates pluripotency and differentiation responses downstream of Erk MAP kinase, Proc. Natl. Acad. Sci. U.S. A. 111 (2014) E1740–E1748.
[9] P. Kovarik, A. Bestehorn, J. Fesselet, Conceptual advances in control of inflammation by the RNA-binding protein tristetraprolin, Front. Immunol. 12 (2022) 751313.
[10] S. Makita, H. Takatori, H. Nakajima, Post-transcriptional regulation of immune responses and inflammatory diseases by RNA-binding ZFP36 family proteins, Front. Immunol. 12 (2021) 711633.
[11] Z. Zhang, et al., RNA-binding protein ZFP36/TTP protects against ferroptosis by regulating autophagy signaling pathway in hepatic stellate cells, Autophagy 16 (2020) 1482–1505.
[12] C.J. Loveridge, S. Slater, K.J. Campbell, N.A. Nam, J. Knight, I. Ahmad, et al., BRF1 accelerates prostate tumourigenesis and perturbs immune infiltration, Oncogene 39 (2020) 1797–1806.
[13] A. Rizzo, M. Santoni, V. Mollica, M. Fiorentino, G. Brandi, F. Massari, Microbiota and prostate cancer, Semin. Cancer Biol. 86 (2022) 1058–1065.
[14] A. Rizzo, V. Mollica, A. Cimadamore, M. Santoni, M. Scarpelli, Giunchi Fet al, Is there a role for immunotherapy in prostate cancer? Cells-Basel 9 (2020).
[15] V. Mollica, A. Marchetti, M. Rosellini, G. Nuvola, A. Rizzo, M. Santoni, et al., An insight on novel molecular pathways in metastatic prostate cancer: a focus on DDR, MSI and AKT, Int. J. Mol. Sci. 22 (2021).
[16] V. Mollica, A. Rizzo, M. Rosellini, A. Marchetti, A.D. Ricci, Aet al Cimadamore, Bone targeting agents in patients with metastatic prostate cancer: state of the art, Cancers 13 (2021).
[17] D. Liko, et al., Brf1 loss and not overexpression disrupts tissues homeostasis in the intestine, liver and pancreas, Cell Death Differ. 26 (2019) 2535–2550.
[18] M. Goldberg, A. Njeh, E. Uzunoglu, Is pulp inflammation a prerequisite for pulp healing and regeneration? Mediat. Inflamm. 2015 (2015) 347649.
[19] S. Sismanoglu, P. Ercal, Dentin-pulp tissue regeneration approaches in dentistry: an overview and current trends, Adv. Exp. Med. Biol. 1298 (2020) 79–103.
[20] O. Tecles, P. Laurent, V. Aubut, I. About, Human tooth culture: a study model for reparative dentinogenesis and direct pulp capping materials biocompatibility, J. Biomed. Mater. Res. B Appl. Biomater. 85 (2008) 180–187.
[21] Y. Wu, C. Zhou, X. Tong, S. Li, J. Liu, Histochemical localization of putative stem cells in irreversible pulpitis, Oral Dis. 28 (2022) 1207–1214.
[22] D.J. Alongi, et al., Stem/progenitor cells from inflamed human dental pulp retain tissue regeneration potential, Regen. Med. 5 (2010) 617–631.
[23] L.O. Pereira, et al., Comparison of stem cell properties of cells isolated from normal and inflamed dental pulps, Int. Endod. J. 45 (2012) 1080–1090.
[24] H.Y. Huang, W.C. Wang, P.Y. Lin, C.P. Huang, C.Y. Chen, Y.K. Chen, The roles of autophagy and hypoxia in human inflammatory periapical lesions, Int. Endod. J. (2018) e125–e145. **51Suppl 2**.
[25] L. Zhu, J. Yang, J. Zhang, B. Peng, The presence of autophagy in human periapical lesions, J. Endod. 39 (2013) 1379–1384.
[26] R. Yang, et al., Autophagy plays a protective role in tumor necrosis factor-alpha-induced apoptosis of bone marrow-derived mesenchymal stem cells, Stem Cell. Dev. 25 (2016) 788–797.
[27] Y. Gao, et al., Induction of autophagy protects human dental pulp cells from lipopolysaccharide-induced pyroptotic cell death, Exp. Ther. Med. 19 (2020) 2202–2210.
[28] S. Lei, X.M. Liu, Y. Liu, J. Bi, S. Zhu, X. Chen, Lipopolysaccharide downregulates the osteo-/odontogenic differentiation of stem cells from apical papilla by inducing autophagy, J. Endod. 46 (2020) 502–508.
[29] F. Pei, H. Lin, H. Liu, L. Li, L. Zhang, Z. Chen, Dual role of autophagy in lipopolysaccharide-induced preodontoblastic cells, J. Dent. Res. 94 (2015) 175–182.
[30] E. Delorme-Axford, D.J. Klionsky, Transcriptional and post-transcriptional regulation of autophagy in the yeast Saccharomyces cerevisiae, J. Biol. Chem. 293 (2018) 5396–5403.
[31] C. Bourcier, P. Griseri, R. Grépin, C. Bertolotto, N. Mazure, G. Pagès, Constitutive ERK activity induces downregulation of tristetraprolin, a major protein controlling interleukin8/CXCL8 mRNA stability in melanoma cells, Am. J. Physiol. Cell Physiol. 301 (2011) C609–C618.
[32] C. Tiedje, et al., The RNA-binding protein TTP is a global post-transcriptional regulator of feedback control in inflammation, Nucleic Acids Res. 44 (2016) 7418–7440.
[33] W. Xie, et al., BRF1 ameliorates LPS-induced inflammation through autophagy crosstalking with MAPK/ERK signaling, Genes. Dis. 5 (2018) 226–234.
[34] J. Romanov, et al., Mechanism and functions of membrane binding by the Atg5-Atg12/Atg16 complex during autophagosome formation, EMBO J. 31 (2012) 4304–4317.